Fusion cross section for the weakly bound neutron system ^{11}Be+^{10}Be at energies below and near the Coulomb barrier

B. Imanishi
Institute for Nuclear Study, University of Tokyo, Tanashi, Tokyo 188, Japan

W. von Oertzen
Hahn-Meitner-Institut Berlin and Fachbereich Physik, Freie Universität Berlin, D-14109 Berlin, Germany
(Received 29 March 1995)

The sub-barrier fusion cross section for the weakly bound neutron system ^{11}Be+^{10}Be is discussed in the framework of the coupled-reaction-channel (CRC) approach for the valence neutron in ^{11}Be and in connection with the molecular orbital formation. In the calculation we observe a big enhancement of the fusion process as well as the formation of a covalent molecule (^{10}Be+n+^{10}Be) due to very strong multistep processes in the inelastic and transfer transitions of the active neutron. As a consequence of the strong CRC effects sharp resonances are observed as fine structure of the fusion cross section, in the case that the absorption effects of the internuclear potential are weak.

PACS number(s): 25.70.Jj, 24.10.Eq, 25.60.+v, 25.70.Ef

I. INTRODUCTION

During the past two decades many authors have discussed the enhancement of sub-barrier fusion cross sections observed in heavy ion collisions [1–19] involving light mass nuclei, in particular the role of the active nucleons; namely, the active nucleons are considered to determine the reaction mechanisms through the inelastic excitations and/or the transfer processes between two core nuclei resulting in some cases in a neck formation.

The correlation between the transfer processes and the mechanisms of the fusion process has been discussed by Landowne and Wolter [4], Dasso, Landowne, and Winter [5], Esbensen and Landowne [9], Lilley *et al.* [10], and Rowley and co-workers [11,17] by employing the coupled-reaction-channel (CRC) method. Although the results tend to explain experimental data and in several experiments the correlation is clearly observed, the mechanism of the correlation is not necessarily conclusive from the CRC analysis [8]. One of the reasons is the fact that the multistep transfer effects are not always so strong as to affect the fusion process, especially in the case where the mass ratio of two core nuclei is far different from unity. The ambiguity in the conclusion also comes (although strong CRC effects are observed in several calculations) from the fact that the cross sections for transfer processes are mainly determined by the reactions occurring at distances outside the grazing distance, while the fusion process occurs mainly inside the grazing distance. Such a situation requires one to treat the transfer processes consistently both inside and outside the grazing distance, *by employing as accurate transfer form factors as possible.*

Another effect of channel coupling, which also gives rise to enhanced fusion cross sections, has been discussed in connection with collective excitations. A distinct dependence on the properties of the channels has been found (e.g., Ref. [18]).

We have previously investigated the fusion mechanism in the system ^{13}C+^{12}C [12,16], and in the system ^{13}C+^{16}O–^{12}C+^{17}O [13,16] in connection with the multistep processes of the inelastic transition and the transfers of the valence neutron in ^{13}C (or ^{17}O), by using our formalism based on the CRC method [12]. In these cases the strong CRC effects of the valence particle give rise to an enhanced sub-barrier fusion cross section and can be explained by the formation of the molecular orbitals of the active neutron.

For systems involving weakly bound (exotic) nuclei much more distinctive features of the CRC effects are expected and the formation of nucleonic molecular orbitals may become the dominant effect. The energy-level spacing of the weakly bound nucleon states may be much smaller and furthermore the tails of the wave functions extend far outside the core nuclei [20]. This may give rise to strong multistep processes as well to a strong mixing of the single-particle wave functions even at distances where the two core nuclei are still far apart from each other.

In the present work we discuss the core-symmetric system ^{11}Be+^{10}Be, with the ^{11}Be having a very weakly bound neutron with a large dipole transition probability between the ground state $2s_{1/2}$ and the first excited state $1p_{1/2}$; thus the radioactive nucleus ^{11}Be has two weakly bound valence neutron states (halo states). The neutron has the separation energies 0.503 and 0.183 MeV in the ground and the first excited states, respectively, and the resonance energy for the second excited state is 1.275 MeV (the width is 100 keV). The analysis for the data of the ^{10}Be(d,p) reactions [21] shows that these states are strong single-particle states; $2s_{1/2}$ (ground state), $1p_{1/2}$ (first excited state), and $1d_{5/2}$ (second excited state) with the spectroscopic factors 0.74, 0.64, and 0.64, respectively. Particular attention should be paid to the inversion of the $1p_{1/2}$-$1s_{1/2}$ level ordering. This is probably due to the coupling to the deformed core ^{10}Be, which has a collective 2^+ excitation. The energy level of the $1p_{1/2}$ state *is very close to that of* $2s_{1/2}$ *and also to that of the sharp resonance state of the* $1d_{5/2}$ *configuration.* This situation is expected to give favorable conditions for very strong CRC effects of the direct inelastic and the transfer processes, and particularly for a strong hybridization, i.e., a strong mixing

 © 1995 The American Physical Society

TABLE I. Parameters of the potential $V_{nC}(R)$ between valence nucleon and core nucleus.

$$V_{nC}(R)=\frac{V^{+}[1+(-)^{\pi}]}{2}\frac{1}{1+\exp[(R-R^{+})/a^{+}]}+\frac{V^{-}[1-(-)^{\pi}]}{2}\frac{1}{1+\exp[(R-R^{-})/a^{-}]}$$
$$+(\boldsymbol{l}\cdot\mathbf{s})\frac{1}{R}\frac{d}{dR}\frac{V'}{1+\exp[(R-R')/a']},$$

with $R^{+}=r_0^{+}A^{1/3}$, $R^{-}=r_0^{-}A^{1/3}$, and $R'=r_0'A^{1/3}$.

$\pi=-$			$\pi=+$			$(\boldsymbol{l}\cdot\mathbf{s})$		
r_0^{-} (fm)	a^{-} (fm)	V^{-} (MeV)	r_0^{+} (fm)	a^{+} (fm)	V^{+} (MeV)	r_0' (fm)	a' (fm)	V' (MeV)
1.20	1.0	−40.12	1.20	0.72	−58.22	1.20	0.845	−31.45

of different parity single-particle states [12]. Such hybridization effects have been observed in the system $^{12}C+^{13}C$, and also in the system $^{36}S+^{37}Cl$ between the states in the sd shell and those in the fp shell of ^{37}Cl [22].

The strong CRC scheme of the $^{11}Be+^{10}Be$ system due to the coupling interactions between the motion of the valence particle and the relative motion of nuclei may induce, at low bombarding energies, a doorway state mechanism where sharp and strong resonances can be produced if the internuclear potential is transparent. Such kinds of quasimolecular states have been observed first by Bromley and co-workers [23,24] in the $^{12}C+^{12}C$ system as a typical example. In our calculation for the $^{11}Be+^{10}Be$ system we observe such structures in the fusion cross sections at energies below and near the Coulomb barrier. The fusion cross sections as well as the total reaction cross sections reflect the resonance phenomena nicely, for example, for the $^{12}C+^{12}C$ system by Erb *et al.* [25] and Treu *et al.* [27].

In Sec. II we explain briefly our CRC formalism [orthogonalized CRC (OCRC)] and the definition of the molecular orbitals. The definition of the fusion cross section is given within this formalism. In Sec. III we discuss the CRC effects in the elastic and inelastic scattering of the system $^{11}Be+^{10}Be$ and the results for the fusion cross sections. We observe a distinctive enhancement of sub-barrier fusion cross sections due to very strong CRC effects. We also show the formation of covalent molecular orbitals of the valence nucleon, which is responsible for the enhancement of the fusion cross section. In Sec. IV possible observation of fine structures in the fusion cross sections of this system is discussed for the case of a weakly absorbing internuclear potential. In Sec. V a summary and the conclusion are given.

II. THE OCRC CALCULATION

By using the three channels defined by three states $1p_{1/2}$, $2s_{1/2}$, and $1d_{5/2}$ (resonance state with the width 100 keV) of ^{11}Be, we have carried out the OCRC calculation as well as the molecular orbital analysis [12]. We consider the transfers of the active neutron between two ^{10}Be nuclei as well as the elastic and inelastic transitions. We have thus the case of nucleon exchange between identical cores, i.e., elastic and inelastic transfers [26]. The wave functions of the single-particle states of the neutron are generated by adjusting the parameters of a Woods-Saxon potential so as to reproduce the binding energies or the resonance energy; the parameters for this potential are listed in Table I. The wave function of the resonance state, the $1d_{5/2}$, is replaced by a wave packet by integrating the scattering waves with the interval of the resonance width (100 keV). The Woods-Saxon potential obtained by this procedure is used as the interaction V_{nC_1} (or V_{nC_2}) causing the inelastic transitions and the transfers of the neutron.

For the interaction between two core nuclei ^{10}Be a Woods-Saxon shape optical potential V_{CC} is taken, with the parameters which are listed in Table II. The real part is almost the same as used in the analysis of the $^{13}C+^{12}C$ system [12]. As for the imaginary part, we use several values of $W=-2$ to -0.2 MeV and later (Sec. IV) a very small depth, $W=-0.1$ MeV. Because all other directly coupled channels than the ones explicitly employed in the present CRC calculation are almost closed at energies below and near the Coulomb barriers, we discuss the possible existence of resonances. As seen later, the overall behavior of the excitation function of the sub-barrier fusion cross section is rather independent of the choice of the potential parameters.

We use an effective Hamiltonian $\mathscr{H}$, which is an approximation of the complete Hamiltonian, $\mathbf{H}=T(r)+T(R)+V_{nC_1}+V_{nC_2}+V_{CC}$, where $T(r)$ and $T(R)$ are the kinetic-energy operators for the relative distance r between two nuclei and for the distance $\mathbf{R}$ between the neutron and core nucleus, respectively. The effective Hamiltonian $\mathscr{H}$ is introduced in the space of the *orthogonalized* basis functions $\phi_i^{JM\Pi}(r,\tau)$, which are defined as

$$\phi_i^{JM\Pi}(r,\tau)=\sum_j \hat{\phi}_j^{JM\Pi}(\hat{\mathbf{r}}',\zeta')N_{ji}^{-1/2}(r',r)$$

with $\tau=(\mathbf{r}',\zeta')$, (1)

TABLE II. Parameters of the optical potential $V_{CC}(r)$. $V_{CC}(r)=V_0/\{1+\exp[(r-R)a]\}+W/\{1+\exp[(r-R_I)/a_I]\}+V_{\mathrm{Coul}}(r_c)$, with $R=2r_0A^{1/3}$ and $R_I=2r_IA^{1/3}$.

r_0 (fm)	a_0 (fm)	V_0 (MeV)	r_I (fm)	a_I (fm)	W (MeV)	r_C (fm)
1.40	0.50	−17.0	1.35	0.35	−1.0	1.35

where $\hat{\phi}_j^{JM\Pi}(\hat{\mathbf{r}}',\zeta')$ are the channel wave functions used in the conventional CRC theory, specified by a set of quantum numbers i and $(JM\Pi)$. The quantities J, M, and Π are the total angular momentum of the system, its Z components, and the total parity, respectively. These quantities will be omitted later as long as there is no source of confusion. The quantity $\hat{\mathbf{r}}'$ is the angular part of the distance vector $\mathbf{r}'$, and ζ' represents all coordinates of the system besides $\mathbf{r}'$. The quantity τ stands for all the coordinates needed to describe the system. If the channel wave functions $\hat{\phi}_i$ and $\hat{\phi}_j$ belong to channels of different mass partitions, they are nonorthogonal and their overlap integral is expressed by $N_{ij}(r',r)$.

We represent the Hamiltonian $\mathscr{H}$ in the space of orthogonalized basis functions $\{\phi_i\}$, and make the following approximation for the interactions (the detailed discussion is given in Ref. [12]):

(i) We drop the interaction terms which are $O((N-I)^2)$, where N is the overlap integral;

(ii) We make a local approximation for the nonlocal transfer interaction $N^{-1/2}(F+F^T)N^{-1/2}/2$, where F is the transfer form factor used in the conventional distorted-wave Born approximation (DWBA) theory.

With the use of the above assumptions we define, in the space of $\{\phi_i\}$, the new effective Hamiltonian $\mathscr{H}$ which contains the interactions only in a local form. In spite of the local approximation the recoil effects occurring in the transfers are approximately included in the $\mathscr{H}$. *We adopt the Hamiltonian $\mathscr{H}$ to obtain solutions of the CRC equation as discussed in the following.*

Molecular orbital states $\Phi_p^{JM\Pi}(r)$ are defined as the eigenstates given by the following equation:

$$[\mathscr{H}(r)-\mathbf{t}(r)]\Phi_p^{JM\Pi}(r)=\mathscr{V}_p^{J\Pi}(r)\Phi_p^{JM\Pi}(r), \tag{2}$$

where $\mathbf{t}(r)$ is the *radial* kinetic-energy operator of the relative motion. They can also be expressed by the previously used basis functions [Eq. (1)] by the transformation

$$\Phi_p^{JM\Pi}(r)=\sum_j \phi_j^{JM\Pi}(r)A_{jp}^{J\Pi}(r). \tag{3}$$

With these channel basis functions $\phi_i^{JM\Pi}(r)$, the transformation coefficients $A_{jp}^{J\Pi}(r)$ are obtained by the following diagonalization:

$$\{[A^{J\Pi}(r)]^{-1}[\mathscr{H}^{J\Pi}(r)-t(r)]A^{J\Pi}(r)\}_{pq}=\mathscr{V}_p^{J\Pi}(r)\delta_{pq}, \tag{4}$$

where the quantity $\mathscr{H}^{J\Pi}$ is the representation of $\mathscr{H}$ in the space of $\{\phi_i^{JM\Pi}\}$. Since the basis functions $\phi_j^{JM\Pi}$ consist of single-particle states of the nucleon, the states $\Phi_p^{JM\Pi}$ are expressed as linear combinations of single-particle nuclear orbitals (LCNO's) [26] combined with the wave functions for the relative rotational motion. *The mixing coefficients $A_{jp}^{J\Pi}(r)$ are dynamically defined by Eq. (4) with the inclusion of the rotational coupling and of the transfer recoil effects*, since the operator $[\mathscr{H}(r)-\mathbf{t}(r)]$ in Eq. (4) contains them.

Reflecting this, the $\Phi_p^{JM\Pi}$ depend on the total angular momentum J and these states are mixed states in the K quantum number (which is the projection of J on the molecular axis). The coupling interactions between different molecular orbital states (radial couplings) are caused by the radial kinetic-energy operator. We call the $\Phi_p^{JM\Pi}$ rotating molecular orbital (RMO) states or dynamically defined LCNO's (DLCNO's). A RMO state $\Phi_p^{JM\Pi}$ agrees with a channel wave function $\hat{\phi}_i^{JM\Pi}$ in the asymptotic region. Therefore the adiabatic potential $\mathscr{V}_p^{J\Pi}(r)$ is regarded as an effective potential describing the elastic scattering of a channel i, if the radial couplings can be neglected, that is, if the radial motion is slow enough.

Various coupling effects are observed in the present OCRC study; enhanced transfers and inelastic cross sections, and enhanced fusion cross sections for energies below the Coulomb barrier. We use the usual definition of the fusion cross section, which is due to the not explicitly coupled channels.

The fusion cross section $\sigma_{\rm fus}$ is defined as [8]

$$\sigma_{\rm fus}=\sum_{J\Pi}\sigma_{\rm fus}^{J\Pi}, \tag{5}$$

$$\sigma_{\rm fus}^{J\Pi}\equiv-\frac{2\pi}{k_1^2}\sum_j\langle u_{j1}^{J\Pi(+)},W_j u_{j1}^{J\Pi(+)}\rangle$$

$$=\sigma^{J\Pi}({\rm abs})-\sum_i\sigma_i^{J\Pi}({\rm reac}), \tag{6}$$

which is the absorption cross sections produced by the imaginary parts $W_j(r)$ of the core-core potential $V_{CC}(r)$ contained in the effective Hamiltonian $\mathscr{H}^{J\Pi}$. The wave functions $u_{j1}^{(+)}(r)$ are the CRC solution of channel j with the incident wave boundary condition for channel 1, and k_1 the wave number of the incident wave.

III. RESULTS OF THE CALCULATION

A. Angular distributions

In Figs. 1 and 2 we show differential cross sections for two energies ($E_{\rm c.m.}$=2.5 MeV at the barrier, and 5.0 MeV). The calculations are carried out by using the optical potentials with imaginary depths $W=-1.0$ and -2.0 MeV for $E_{\rm c.m.}$=2.5 and 5.0 MeV, respectively. The figures show for the elastic channel the strong backward rises due to the transfer processes mainly coming from the first order perturbation (one-step DWBA) term in the $2s_{1/2}$ ground-state channel, which is particularly pronounced for the higher energy.

In the figures we also show the calculation corresponding to the one-step DWBA. The CRC effects are observed by an enhancement of the elastic and transfer transitions; generally this enhancement is connected with a shift of the maximum in angle. These angle shifts in the transfer processes [^{10}Be(^{11}Be,^{10}Be)^{11}Be$^{(*)}$] which are observed at backward angles in the angular distributions (at $180°-\theta_{\rm c.m.}$) indicate that the reaction proceeds at rather large distances. This is of course due to the long range of the single-particle wave functions, the $1p_{1/2}$, $2s_{1/2}$, and $1d_{5/2}$ states of the active nucleon in ^{11}Be, which have very similar radial extension.

We can discuss this effect by using the semiclassical relation for minimum distance R and scattering angle θ ($R=(\eta/k)[1+\sin^{-1}(\theta_{\rm c.m.}/2)]$; k is the wave number of the radial relative motion and η the Sommerfeld parameter). We obtain a typical distance of R=17–20 fm (at $E_{\rm c.m.}$=5 MeV) for the grazing peak in the first order result and a shift to distances R=23–25 fm for the OCRC calculation (for a

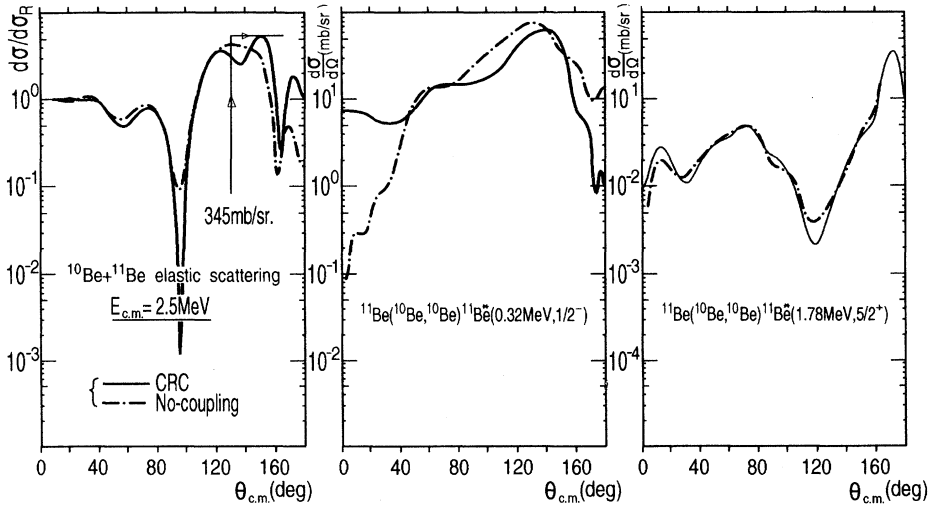

FIG. 1. Angular distributions obtained for the scattering of ^{11}Be on ^{10}Be using the CRC calculations at $E_{\text{c.m.}}=2.5$ MeV. The full curve shows the complete calculation; the dot-dashed curve the result obtained by one-step DWBA.

grazing angle maximum at $\theta_{\text{c.m.}}=15°$). The same holds for the case of $E_{\text{c.m.}}=2.5$ MeV (with a shift in grazing angle from $\theta_{\text{c.m.}}=45°$ to 30°). At $E_{\text{c.m.}}=2.5$ MeV the contributions to the S matrix extend to rather large angular momentum J of the total system; these are, however, not easily observed in the angular distributions of the elastic scattering.

In contrast to the differential cross sections the fusion cross sections show strong CRC effects especially at lower energies, as discussed in the following subsection III B. This suggests that the CRC effects observed in the differential cross sections are due to reaction mechanisms which are different from those observed in the fusion cross sections; namely, *the fusion cross sections reflect absorption due to the optical potential inside of the potential barrier, as seen from Eq. (6), while the differential cross sections reflect the reaction mechanisms outside the barrier.*

The inelastic transitions at forward angles are generally also enhanced by the CRC effects.

Further, the influence of the imaginary potential has been studied; the general result is that from values larger than $W=-0.5$ MeV the result is not changed any more with increasing value of W although the convergence of the higher multistep DWBA is strongly influenced. Other, smaller values of W and a larger value with small radial parameter are discussed in Sec. IV.

B. Fusion cross sections

In this subsection we discuss the CRC effects on the fusion cross sections and the reaction mechanism, and clarify the role which the valence neutron in ^{11}Be plays in the fusion processes.

In Fig. 3(a) the OCRC calculation of σ_{fus} (the solid curve) with the use of the optical potential with an imaginary part of $W=-0.2$ MeV is compared, as a function of the incident energy $E_{\text{c.m.}}$, with the one-channel calculation (the dash-dotted curve) which is obtained by employing the full interaction potential including the elastic direct and transfer interactions of the valence nucleon in addition to the core-core optical potential. With increasing energy the OCRC result for

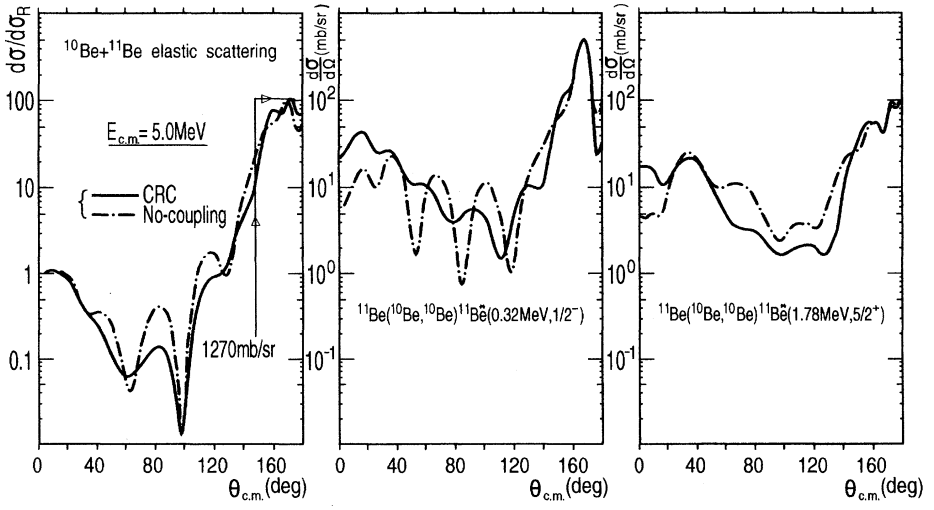

FIG. 2. As Fig. 1 for the energy of $E_{\text{c.m.}}=5$ MeV.

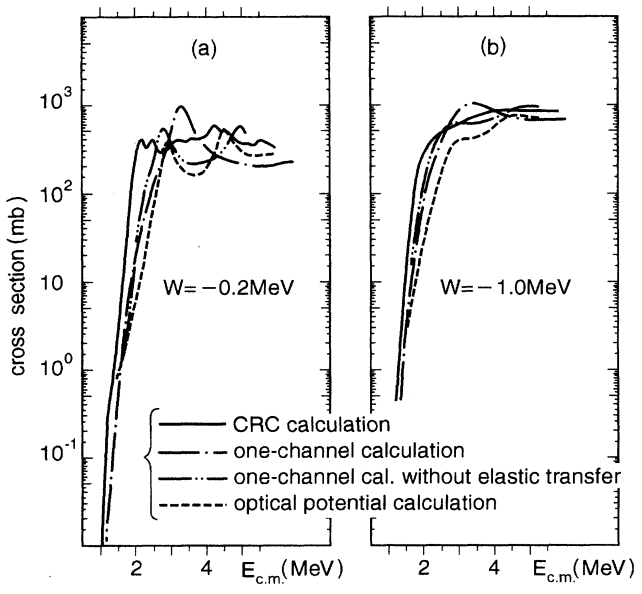

FIG. 3. Excitation functions of the fusion cross sections for the ^{11}Be+^{10}Be system calculated (a) with a weakly absorbing core-core optical potential ($W=-0.2$ MeV) and (b) with a stronger absorbing potential ($W=-1.0$ MeV). The solid curves show the CRC calculation, the dash-dotted curves a one-channel calculation with the full interaction (core-core optical potential + the direct folding potential + the elastic transfer interaction), and the dash-two-dotted curves a one-channel calculation with the interaction obtained by removing the elastic transfer interaction from the full interaction. The dashed curves show the optical model calculation with the same optical potential as the core-core potential but obtained by slightly changing the radius parameters so as to fit to the size of the system ^{10}Be+^{11}Be.

$\sigma_{\rm fus}$ rises very sharply and saturates at about 2 MeV, while in the no-coupling calculation the rise is slower and it saturates at about 3 MeV. Clearly the CRC effects enhance $\sigma_{\rm fus}$ at energies below the Coulomb barrier. This mechanism is discussed later in relation to hybridization effects on the molecular orbital formation of the valence neutron.

The dashed curve in the figure shows the calculation only with the use of almost the same core-core (^{10}Be-^{10}Be) optical potential as used in the OCRC analysis but obtained by slightly changing the radius parameters of the real and imaginary parts into $r_0=1.372$ fm and $r_I=1.423$ fm so as to fit the size of the system ^{11}Be+^{10}Be (not the size of the system ^{10}Be+^{10}Be). If the valence neutron behaves as if it were a nucleon as in the core nucleus ^{10}Be, the fusion cross section should be estimated by this optical potential alone. As seen from the comparison of this curve with the dash-dotted curve, however, this optical potential model underestimates completely the fusion cross section at energies below and near the Coulomb barrier, that is, the valence neutron contributes to the enhancement of the fusion cross section even in the one-channel framework by the direct folding potential and the elastic transfer interaction of the weakly bound $2s_{1/2}$ channel.

The dash-two-dotted curve in the figure shows the result of the one-channel calculation by using the core-core optical potential plus the direct folding potential of the valence nucleon alone, i.e., the one-channel calculation omitting the elastic transfer interaction from the full interaction. The result of this calculation is not so different from that of the full one-channel calculation (the dash-dotted curve), suggesting that *the elastic transfer interaction is not the major part of the interaction responsible for the enhancement of the fusion cross section.* This means that the enhancement of the fusion cross section, which is seen by the comparison of the full interaction calculation (the dash-dotted curve) to the above optical model calculation (the dashed curve), is due to the direct folding potential of the valence neutron. Such a fact has also been pointed out by Takigawa and Sagawa in their study [19] for the system ^{11}Li+^{9}Li.

The peaks and the valleys observed in the OCRC calculation come from the resonances of the scattering system ^{11}Be+^{10}Be. This is discussed in the next section in detail, where also examples with $W=-0.1$ and -0.5 MeV and with $W=-1$ MeV with small radial parameter are shown.

In Fig. 3(b) the calculations with a much stronger absorption potential are shown. In spite of the change of the imaginary depth of the core-core potential ($W=-1.0$ MeV) the general behavior of $\sigma_{\rm fus}$ is the same as in the calculation with $W=-0.2$ MeV. That is, the enhancement of the fusion cross section at sub-barrier energies is observed independently from the potential absorption.

In order to discuss the mechanism of the enhancement observed in the above calculation, we employ the RMO model defined by Eqs. (2) and (4). The adiabatic potentials $\mathscr{V}_p^{J\Pi}(r)$ calculated are shown in Fig. 4 for the case of $J^\Pi=7/2^+$, and are compared with the incident-channel bare potential $U_{11}(r)$ contained in the Hamilton $\mathscr{H}$ [it should be noted that the elastic transfer interaction in the incident channel is included in the potential $U_{11}(r)$]. As seen in the figure, the ground-state adiabatic potential $\mathscr{V}_{p=1}(r)$, which agrees with $U_{11}(r)$ in the asymptotic region, is much lower than $U_{11}(r)$ in the interaction region. The difference is about 1 MeV at the distance $r=8$ fm (at the potential barrier top) where the overlap of the densities of the two core nuclei is still small. Furthermore, this lowest adiabatic potential $\mathscr{V}_{p=1}(r)$ is isolated far from other adiabatic potentials in the grazing region, suggesting that the lowest molecular orbital state is adiabatically stable with respect to the radial motion.

The energy difference of 1 MeV between $U_{11}(r)$ and $\mathscr{V}_{p=1}(r)$ at the barrier top explains the energy shift of the CRC calculation for the excitation functions of $\sigma_{\rm fus}$ relative to the no-coupling calculations but with the inclusion of the elastic transfer interactions.

The adiabatic potential $\mathscr{V}_{p=1}(r)$ shows outside the barrier top a much more flattened shape than the potential $U_{11}(r)$. This explains the sharp rise of the OCRC calculation of the excitation function of $\sigma_{\rm fus}$.

Essential features of the CRC effects can be discussed in the present method by the inspection of the density distribution of the valence neutron, which can be plotted by using the functions $\Phi_p^{JM\Pi}$ with the core-core distance r as a parameter (see the upper part of Fig. 4).

The lowest RMO state $\Phi_{p=1}^{JM\Pi}$ shows the characteristic feature of the density distribution of the active neutron reflecting the attractive interactions between the neutron and the core nuclei. As shown in Fig. 4, a very distinctive cova-

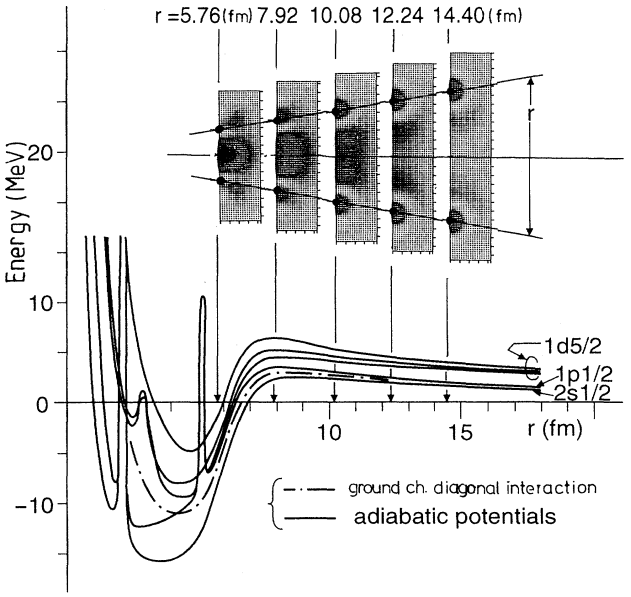

FIG. 4. Adiabatic calculations for the ^{11}Be+^{10}Be system in the state $J^{\Pi}=7/2^{+}$. In the lower part of the figure the adiabatic potentials are shown by the solid curves and the incident-channel diagonal potential $U_{11}(r)$ between ^{11}Be and ^{10}Be by the dash-dotted curve. The potential U_{11} includes all the interactions for the channel 1, i.e., the core-core potential, the direct folding potential, and the elastic transfer interaction. In the upper part the density distributions of the active neutron in the ground RMO state are shown at several points of the radial distance larger than the grazing distance.

lent molecule, ^{10}Be+n+^{10}Be, is already formed at large distances outside the Coulomb barrier. The neutron density concentrates in the middle of the axis joining the two centers of the core nuclei. In Fig. 5 the mixing coefficients $A^{J\Pi}_{ip=1}(r)$ for $p=1$ corresponding to the above covalent molecular orbital state are shown as a function of distance r, where the coefficients with $K=1/2$ (the projection of the total angular momentum J on the molecular axis) dominate. We see clearly that this covalent molecule is very stable for the rotational motion of the system in the grazing region, because the RMO state is almost pure in the K quantum number of $K=1/2$.

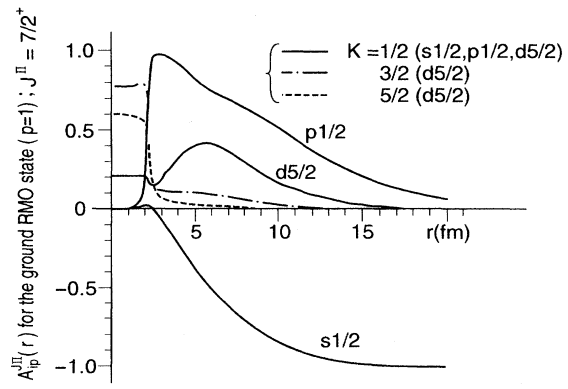

FIG. 5. Mixing coefficients $A^{J\Pi}_{ip}(r)$ for the ground RMO state ($p=1$) of the ^{11}Be+^{10}Be system in the state $J^{\Pi}=7/2^{+}$. The solid curves show the components of $K=1/2$ for the single-particle states $2s_{1/2}$, $1p_{1/2}$, and $1d_{5/2}$. The dash-dotted and the dotted curves are the components of $K=3/2$ and 5/2 of the $1d_{5/2}$ state, respectively.

IV. CALCULATION USING WEAKLY ABSORBING POTENTIALS: RESONANCES

In this section we discuss the result of OCRC calculations with a weakly absorbing potential, where we observe many structures in the excitation function of the fusion cross sections. We also test a core-core optical potential, which is again transparent at the surface region, but strongly absorptive in the inside region determined by the radius parameter $r_I=1.0$ fm. This type of potential is often used in discussions of fusion cross sections.

Since quasimolecular states have been observed by Bromley and co-workers in the scattering of ^{12}C on ^{12}C [23,24], many resonance phenomena in a large variety of heavy ion collisions have been reported [24]. Among the many resonance systems investigated, the ^{12}C+^{12}C system at low energies near or below the Coulomb barrier has shown the most conspicuous phenomena, that is, the resonances are very sharp (widths ~100–150 keV) and are clearly isolated from each other. These quasimolecular states can be interpreted as the doorway states induced by strong coupling interactions between two ^{12}C nuclei [28–32] and are supported by a scheme where the incident flux is only weakly absorbed [29,33,34]; namely, the bare interaction potential between two ^{12}C nuclei, as it occurs in the calculation, is so transparent that the dinuclear molecular resonance states can live for such a long time as estimated from the narrow resonance widths observed.

We are here concerned with a system where the coupling of the valence particle to the motion of the relative distance could induce a sufficiently strong coupling as to produce similar effects to those of the 2^{+} excitation of ^{12}C. In a variety of systems indications for such resonances have been searched for [35–37]. However, no clear indication has been observed.

In the scattering of the ^{13}C+^{13}C system Korotky *et al.* have discussed the possible existence of molecular orbitals of the active neutron [38]. For this system Terlecki, Scheid, and Greiner [39], Koennecke, Greiner, and Scheid [40], and Thiel *et al.* [41] have made extensive molecular orbital calculations by using the particle-core model [42] based on the two-center shell model, and have obtained agreement with some structures in the data. The method of the neutron molecular orbitals model has been also applied to the system ^{17}O+^{12}C–^{16}O+^{13}C by Thiel, Greiner, and Scheid [43] in the analysis of the data of Ref. [44].

In previous work we have performed the analysis of the experimental data for systems with one valence nucleon, like ^{12}C+^{13}C, ^{13}C+^{16}O–^{12}C+^{17}O, and ^{36}S+^{37}Cl, with the use of the OCRC theory developed in Ref. [12]. Nonetheless, resonance states have not been observed in these systems, probably because the coupling effects are not strong enough at the nuclear surface, and the motions of the valence nucleon couple to the collective motions of core nuclei strongly in some cases only; this may give large widening and splitting

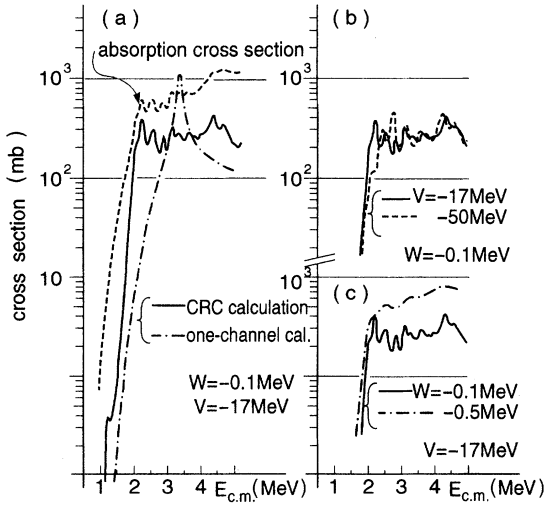

FIG. 6. Excitation functions of the fusion cross sections of the ^{11}Be+^{10}Be system and the absorption cross section [the dotted curve in (a)]. The solid and the dash-dotted curves in (a) are the CRC calculation of the fusion cross sections and one-channel (no-coupling) calculation, respectively. In (b) and (c) the solid curves are the same one as in (a). The dotted curve in (b) and the dash-dotted curve in (c) show the calculations with the real depth $V_0=-50$ MeV of the core-core potential and with the imaginary depth $W=-0.5$ MeV, respectively.

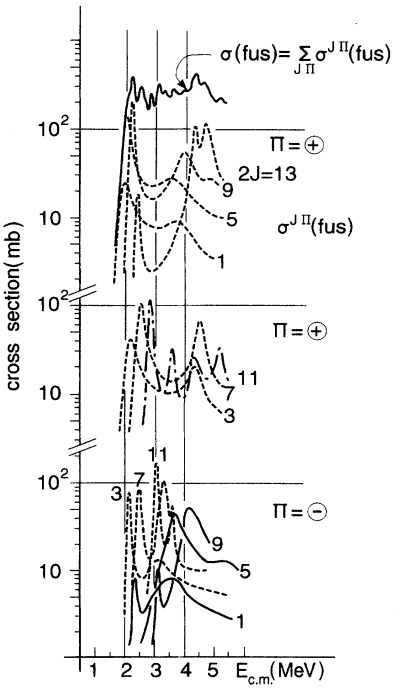

FIG. 7. Partial fusion cross sections $\sigma_{\rm fus}^{J\Pi}$ and the total fusion cross section $\sigma_{\rm fus}$. The number attached to each partial fusion cross section denotes twice the total angular momentum J.

effects on the resonances formed in such single-particle coupled-reaction-channel systems.

In the present case of the ^{11}Be+^{10}Be system, the channels concerned with the *single-particle states of the valence neutron* in ^{11}Be are at *very low excitation energies*, while the channels concerned with the *collective core excitation* of ^{10}Be are *higher* and more isolated from the incident channel.

The fusion cross section is a proper quantity to see the resonance effects, especially when the main part of the flux absorbed from the incident channel is in the reaction cross sections calculated by the CRC calculation, and the smaller part is due to the absorption via the imaginary part of the core-core potential. As seen from Eq. (2), $\sigma_{\rm fus}$ reflects the scattering wave functions which take large amplitudes in the interaction region at resonance energies.

In Fig. 6 results with one channel and the complete OCRC calculations are shown for an imaginary potential with $W=-0.1$ MeV. We see pronounced fine structure in the OCRC calculation (solid curve) of the excitation function of $\sigma_{\rm fus}$, which consists of different partial cross sections $\sigma_{\rm fus}^{J\Pi}$. The one-channel calculation shows one prominent potential resonance which is damped with increasing strength of the imaginary part of the potential (see also Fig. 3).

In Fig. 7 the values for $\sigma_{\rm fus}^{J\Pi}$ are shown for $J^{\Pi}=1/2^{+}-15/2^{+}$ and $1/2^{-}-13/2^{-}$. Very sharp peaks are observed together with broad bumps. Among these peaks the larger ones contribute to the appearance of fine structure of $\sigma_{\rm fus}$.

As seen in Fig. 7, however, the partial cross section of not only one J^{Π} value necessarily contributes to one peak observed in $\sigma_{\rm fus}$. Sometimes one sharp peak is obtained by the superposition of several different partial cross sections.

The dash-dotted curves in Fig. 6(a) shows the $\sigma_{\rm fus}$ calculated by using the incident channel only (one-channel calculation; the direct folding potential and the elastic transfer interaction are included as stated in Sec. III). No fine structure is observed there; the large bump comes from several resonances belonging to different sets of J and Π. The comparison of this result with the OCRC calculation suggests that the fine structures obtained by the OCRC calculations of $\sigma_{\rm fus}$ and the $\sigma_{\rm fus}^{J\Pi}$ come from resonances which correspond to the doorway states of a two-center system defined in the CRC scheme adopted here.

The behavior of the excitation functions of $\sigma_{\rm fus}$ and $\sigma_{\rm fus}^{J\Pi}$ depends clearly on the choice of the parameters of the core-core potential V_{CC}. In Fig. 6(b) the calculation of $\sigma_{\rm fus}$ with the depth $V_0=-50$ MeV (dashed curve) is compared to the calculation (solid curve) with the standard depth ($V_0=-17$ MeV). The resonance structure and so the positions of the resonance energies are changed due to the change of the real depth V_0; however, the fine structure itself persists as in the calculation with the shallow potential. This means that the formation mechanism of the above resonances is determined not by the interaction potential V_{CC} between two ^{10}Be nuclei but by the interactions V_{nC_i} ($i=1$ and 2), which cause strong couplings between different single-particle channels through the inelastic transitions and the transfers of the active neutron.

Fusion mechanisms induced by heavy ion collisions have often been discussed by many authors under the concept that the fusion occurs inside a small internuclear distance with large overlap of two colliding nuclei. In this context we examine the possibility of resonances by using the optical po-

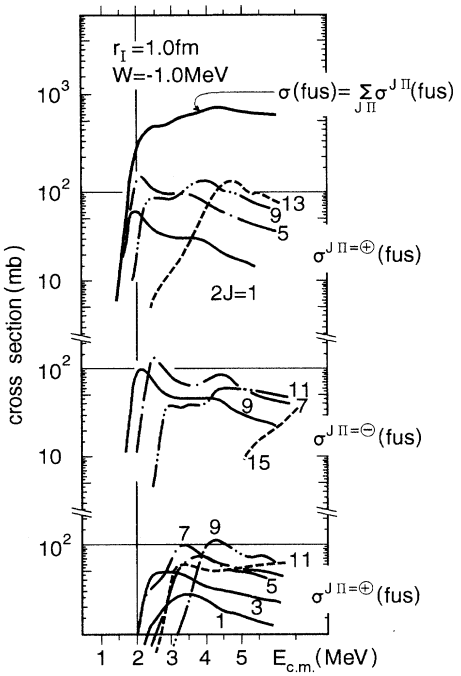

FIG. 8. As Fig. 7 but with the use of the core-core optical potential with a small radius parameter and a deeper depth for the imaginary part (see text).

tential which has the same real part as used in the above discussion and an imaginary part with a small radius parameter of $r_I = 1.0$ fm and stronger absorption of $W = 1.0$ MeV.

As shown in Fig. 8, the prominent fine structures observed in the calculation of σ_{fus} obtained with the use of the weakly absorbing optical potential are clearly damped by the absorption inside the small radius. Nevertheless, however, we still find some indications of the structures, especially in the partial fusion cross sections. Such appearance is due to the strong channel couplings in the surface region caused by the long-range wave functions of the valence neutron.

In light heavy ion collisions at energies near the Coulomb barrier the role of the Pauli principle between nucleons belonging to different colliding nuclei is very important. This effect can be effectively replaced by a repulsive core interaction in an optical potential with spatially local form. This repulsive core may work so as to prevent absorption of incident flux in the region where the overlap of two colliding nuclei becomes larger. If such circumstances can be provided for the system ^{10}Be+^{10}Be we have a possibility to observe again fine structures in the fusion cross sections.

The result of the OCRC calculations clearly shows that the resonances depend in their widths on the strength of the imaginary potential, that is, the width increases with the increase of W; this means that the coupling responsible for the occurrence of the splitting of the individual resonances observed in Fig. 7 happens inside the barrier. This effect can be seen to be due to the very strong coupling of the $2s_{1/2}$ state to the $1p_{1/2}$ (and partially to the $1d_{5/2}$) state, the long-range form factors thus give a mixing of the $2s_{1/2}$ and $1p_{1/2}$ states over a long range of distances (see Fig. 5).

V. SUMMARY AND DISCUSSION

We summarize the result of the OCRC calculation for the ^{11}Be+^{10}Be system by finding that the CRC interactions concerned with very weakly bound states $2s_{1/2}$ and $1p_{1/2}$ and with the sharp resonance state $1d_{5/2}$ of the active neutron in ^{11}Be induce a big enhancement of the sub-barrier fusion cross section. This is due to the transfer and inelastic couplings to the $1p_{1/2}$ and $1d_{5/2}$ states and due to the formation of covalent molecular orbital states. The barrier height of the adiabatic potential corresponding to this molecular orbital state is much lower than the bare potential between ^{11}Be and ^{10}Be by about 1 MeV. Such strong coupling effects especially in the grazing region come from (i) long tails of the wave functions of the valence halo neutron in ^{11}Be employed in the OCRC calculation, (ii) narrow energy-level spacing of the neutron single-particle states, and (iii) strong mixing of different l-parity states, i.e., the hybridization of the p and sd states.

For the formation of the lowest energy state the mixing of the $2s_{1/2}$ and $1p_{1/2}$ states is most important, as can be seen in Fig. 5. This mixing of states of opposite parity is essential for the observation of the enhancement.

In the CRC calculations for the ^{13}C+^{12}C system in Refs. [12] and [16], we also observed coupling effects similar to those for the system ^{11}Be+^{10}Be but they were not as strong as seen in the case of ^{11}Be+^{10}Be, especially outside the potential barrier. The valence neutron in ^{13}C has the same single-particle states as in ^{11}Be but with larger binding energies, particularly for the $1p_{1/2}$ state. The large binding energy of 4.946 MeV for the $1p_{1/2}$ state in ^{13}C and the large energy-level spacing between the p and sd states gave less favorable conditions for strong hybridization and a strong CRC scheme than observed in the ^{11}Be+^{10}Be system.

Bertulani and Balantekin [14] have also pointed out that the enhancement of the fusion cross section in the system ^{9}Li+^{11}Li is obtained as the result of the molecular bond effects of the (two) valence neutrons in ^{11}Li. *However, this is not the CRC effect discussed in this report.* On the contrary, the elastic transfer interaction, to which Bertulani and Balatekin have paid attention, plays a rather minor role in the enhancement phenomena of the fusion cross section of the system ^{11}Be+^{10}Be. Probably, in their work the main part of the molecular bond effects comes from the direct folding potential of the interaction V_{nC}, as pointed out by Takigawa and Sagawa [19]. That is, the molecular bond effects, which they have discussed, are not the effects from the formation of the molecular bonds which depend on hybridization just as in atomic molecules. In our calculation the channel-diagonal potential already includes these folding effects.

The resonances in σ_{fus} appear if a fairly transparent optical potential between two ^{10}Be nuclei is used, which makes the predicted resonance widths narrow. These resonances are considered to be doorway states, which appear due to the strong CRC scheme of the single-particle channels with the weakly bound states. A one-channel calculation does not produce the fine structure as observed in the CRC calculation. The strong couplings are induced by a very strong polarization of the single-particle orbit (the hybridization), i.e., the mixing of the different-parity single-particle states and the strong multistep transfers are enhanced by the hybridization

[12,22]. As shown in the discussion of the enhancement of the sub-barrier fusion cross section, the barrier height is effectively lowered by the CRC effects and the incident waves penetrate into the interior of the potential even at sub-barrier energies. Thus the sharp resonances can be observed even at fairly low energies below the barrier as the doorway states for the ground-state covalent-molecular channels.

We tested the resonance phenomena also by using a core-core optical potential which has a strong imaginary part inside the radius corresponding to the so-called fusion radius parameter $r_I=1.0$ fm, where the fusion is assumed to occur strongly. The result of this calculation shows that there is no prominent structure any more in the excitation function of the fusion cross section, although the signature of the structures remains there, probably coming from the strong channel couplings at the surface region.

The resonances due to the formation of covalent molecules may further appear as much broader resonances above the Coulomb barrier. A detailed analysis along the lines of the molecular orbital model is in progress.

ACKNOWLEDGMENTS

The authors wish to thank Professor H. H. Wolter for his discussion on the effects of multistep processes with weakly bound single-particle states of the active nucleon. Helpful conversations are gratefully acknowledged with Professor T. Nomura and Professor R. H. Siemssen. The authors are also indebted to Dr. Izumoto for his helpful assistance to improve a computer program at an earlier stage of the research. One of the authors (B.I.) wishes to thank the members of the HMI for their hospitality during his stay there. This research was supported by Japan Society of Promotion of Science under a grant for international scientific collaboration research. The calculation was performed at the computer centers of INS and HMI.

[1] R. G. Stokstad, Z. E. Switkowski, R. A. Dayras, and R. M. Wieland, Phys. Rev. Lett. **37**, 888 (1976); R. A. Dayras, R. G. Stokstad, Z. E. Switkowski, and R. M. Wieland, Nucl. Phys. **A265**, 153 (1976).

[2] S. Dasmahapatra, B. Čujec, and F. Lahlou, Nucl. Phys. **A384**, 257 (1982); M. L. Chatterjee, L. Potvin, and B. Čujec, *ibid.* **A333**, 273 (1980).

[3] C. T. Papadopoulos, R. Vlastau, E. N. Gazis, P. A. Assimahopoulos, C. A. Kalfas, S. Kossionides, and A. C. Xenoulis, Phys. Rev. C **34**, 196 (1986); B. Dasmahapatra, B. Čujec, I. M. Szöghy, and J. A. Cameron, Nucl. Phys. **A526**, 395 (1991); R. J. Tighe, J. I. Kolata, and M. Belbot, Phys. Rev. C **47**, 2699 (1993).

[4] S. Landowne and H. H. Wolter, Nucl. Phys. **A351**, 171 (1981).

[5] C. H. Dasso, S. Landowne, and A. Winter, Nucl. Phys. **A405**, 381 (1983).

[6] A. M. Stefanini *et al.*, Phys. Lett. B **185**, 15 (1987).

[7] P. H. Stelson, Phys. Lett. B **205**, 190 (1988); P. H. Stelson, H. J. Kim, M. Beckerman, D. Schapira, and R. L. Robinson, Phys. Rev. C **41**, 1584 (1990).

[8] L. Corradi, in Proceedings of the International Workshops on Heavy-Ion Fusion: Exploring the Variety of Nuclear Properties, .Padua, Italy, 1994, edited by A. M. Stefanini *et al.* (unpublished), p. 34.

[9] H. Esbensen and S. Landowne, Nucl. Phys. **A492**, 473 (1989).

[10] J. S. Lilley, M. A. Nagarajan, D. W. Bans, B. R. Fulton, and I. J. Thompson, Nucl. Phys. **A463**, 710 (1987); I. J. Thompson, M. A. Nagarajan, J. S. Lilley, and B. R. Fulton, *ibid.* **A487**, 141 (1988).

[11] N. Rowley, I. J. Thompson, and M. A. Nagarajan, Phys. Lett. B **282**, 2760 (1992).

[12] W. von Oertzen and B. Imanishi, Nucl. Phys. **A424**, 262 (1984); B. Imanishi and W. von Oertzen, Phys. Rep. **155**, 29 (1987).

[13] B. Imanishi, S. Misono, and W. von Oertzen, Phys. Lett. B **241**, 13 (1990).

[14] C. A. Bertulani and A. B. Balantekin, Phys. Lett. B **314**, 275 (1993).

[15] R. R. Betts, in Proceedings of the Symposium on Heavy Ion Interactions around the Coulomb Barrier, Legnaro, Italy, 1988, edited by C. Signorini *et al.* (unpublished), p. 93; in Proceedings of the JAERI International Symposium on Heavy-Ion Reaction Dynamics in Tandem Energy Region, Hitachi, Japan, 1988, edited by Y. Sugiyama *et al.* (unpublished), p. 63.

[16] B. Imanishi and W. von Oertzen, in Proceedings of RIKEN International Workshop on Heavy-Ion Reactions with Neutron-Rich Beams, Wako, Japan, 1993, edited by M. Ishihara *et al.* (unpublished), p. 85.

[17] M. Rowley, I. J. Thompson, and Baggley, in Proceedings of the Workshop on the Physics and Techniques of Secondary Nuclear Beams, Dourdan, France, 1992, edited by J. F. Bruandet, B. Fernandez, and M. Bex (unpublished); N. Rowley, Nucl. Phys. **A538**, 205c (1992).

[18] C. A. Bertulani, L. F. Canto, and M. S. Hussein, Phys. Rep. **226**, 281 (1993).

[19] N. Takigawa and S. Sagawa, Phys. Lett. B **265**, 23 (1991).

[20] D. V. Fedorov, A. S. Jensen, and K. Riisager, Phys. Lett. B **312**, 1 (1993).

[21] F. Ajzenberg-Selove, Nucl. Phys. **A506**, 1 (1990).

[22] R. Bilwes, B. Bilwes, L. Stuttge, J. L. Ferrero, J. A. Ruiz, W. von Oertzen, and B. Imanishi, Phys. Rev. Lett. **70**, 259 (1993).

[23] D. A. Bromley, J. A. Kuehner, and E. Almqvist, Phys. Rev. Lett. **4**, 365 (1960); E. Almqvist, D. A. Bromley, and J. A. Kuehner, *ibid.* **4**, 515 (1960); E. Almqvist, D. A. Bromley, J. A. Kuehner, and B. Whalen, Phys. Rev. **130**, 1140 (1963).

[24] K. A. Erb and D. A. Bromley, in *Treatise on Heavy-Ion Science*, edited by D. A. Bromley (Plenum, New York, 1984), Vol. 3, p. 201; see also references to prior work therein.

[25] K. A. Erb, R. R. Betts, S. K. Korotky, M. M. Hindi, P. P. Tung, M. W. Sachs, S. J. Willett, and D. A. Bromley, Phys. Rev. C **22**, 507 (1980).

[26] W. von Oertzen, Nucl. Phys. **A148**, 529 (1970); W. von Oertzen and H. G. Bohlen, Phys. Rep. **19C**, 1 (1975).

[27] W. Treu, H. Fröhlich, W. Galster, P. Dück, and H. Voit, Phys. Rev. C **22**, 2462 (1980).

[28] E. Vogt and H. McManus, Phys. Rev. Lett. **4**, 518 (1960).

[29] B. Imanishi, Phys. Lett. **27B**, 267 (1968); Nucl. Phys. **A125**, 33 (1969).

[30] G. Michaud and E. W. Vogt, Phys. Rev. C **5**, 350 (1973).
[31] M. Ohkubo, K. Kato, and H. Tanaka, Prog. Theor. Phys. **67**, 207 (1982); K. Kato and H. Tanaka, *ibid.* **81**, 390 (1989).
[32] S. Marsh and W. D. M. Rae, Phys. Lett. B **180**, 185 (1986); J. Zhang and W. D. M. Rae, Nucl. Phys. **A564**, 252 (1993).
[33] Y. Abe, Y. Kondo, and T. Matsuse, Prog. Theor. Phys. Suppl. No. 68 (1980), Chap. 4, p. 303.
[34] F. Haas and Y. Abe, Phys. Rev. Lett. **46**, 1667 (1981); B. Beck, Y. Abe, N. Aissaoui, B. Djerroud, and F. Haas, Phys. Rev. C **49**, 2618 (1994).
[35] R. J. Tighe, J. J. Kolata, and M. Belbot, Phys. Rev. C **47**, 2699 (1993).
[36] A. D. Frawley, N. R. Fletcher, L. C. Dennis, and K. M. Abdo, Nucl. Phys. **A394**, 292 (1983).
[37] G. P. Gilfoyle, J. Richards, and H. T. Fortune, Phys. Rev. C **34**, 152 (1986).
[38] S. K. Korotky, K. A. Erb, R. L. Phillips, S. J. Willett, and D. A. Bromley, Phys. Rev. C **28**, 168 (1983).
[39] G. Terlecki, W. Scheid, and W. Greiner, Phys. Rev. C **18**, 265 (1978).
[40] R. Koennecke, W. Greiner, and W. Scheid, Phys. Rev. Lett. **51**, 366 (1983).
[41] A. Thiel, W. Greiner, J. Y. Park, and W. Scheid, Phys. Rev. C **36**, 647 (1987).
[42] J. Y. Park, W. Scheid, H. J. Fink, and W. Greiner, Phys. Rev. C **6**, 1565 (1972); **20**, 188 (1979).
[43] A. Thiel, W. Greiner, and W. Scheid, J. Phys. G **14**, L85 (1988); A. Thiel, *ibid.* **16**, 867 (1990).
[44] R. M. Freeman, C. Beck, F. Haas, A. Morsad, and N. Cindro, Phys. Rev. C **33**, 1275 (1986); R. M. Freeman, F. Haas, A. Morsad, and C. Beck, *ibid.* **39**, 1335 (1989).